The tripole vortex: Experimental evidence and explicit solutions

Ziv Kizner[1,2,*] and Ruvim Khvoles[2]
[1]*Department of Physics, Bar-Ilan University, 52900 Ramat-Gan, Israel*
[2]*Department of Mathematics and Statistics, Bar-Ilan University, 52900 Ramat-Gan, Israel*
(Received 24 June 2003; published 12 July 2004)

Based on experimental evidence, explicit vorticity-distributed solutions to the Euler equations in two dimensions are constructed describing the tripole vortex. The vortex form and the solution outside the region of nonzero vorticity are derived analytically, while the interior is solved numerically. The continuous-vorticity solution reproduces the main features of the tripoles observed in laboratory experiments and numerical simulations—their shape, flow pattern, and the form of the nonlinear vorticity vs streamfunction relation. The approach followed in the construction of a tripole proves to be beneficial in the search for higher-order multipoles, an example being a smooth quadrupole solution.

DOI: 10.1103/PhysRevE.70.016307 PACS number(s): 47.32.Cc, 52.35.We, 92.10.Fj

I. INTRODUCTION

Localized distributed vortices are common in ordinary fluids and plasmas. In an ideal fluid, any two-dimensional (2D) circularly symmetric monopole represents an exact stationary solution. The first nontrivial vortical solution—the translating circular dipole—was suggested independently about a century ago by Lamb [1] and Chaplygin [2] (see Ref. [3], where Chaplygin's solution is reproduced and analyzed). Since that time, most of the research in the dynamics of localized distributed vortices has been associated with monopoles and dipoles or their combinations. In the last 15 years, the tripole and even more complex rotating vortices marked by zero total circulation have been studied mainly by experimental and numerical methods [4–14], analytical approaches being mostly applied to singular and piecewise-constant vorticity situations (see Refs. [15–19] and references therein).

The emergence of tripoles was first independently observed in numerical simulations [4] and laboratory experiments with *compact isolated* monopoles produced using the stirring technique in a homogeneous rotating fluid (f plane), where weak motions can be regarded as nondivergent and quasi-2D [6,8]. Here, *compact* means that the vorticity differs from zero only within a finite region, while the term *isolated* is used in reference to vortices with zero circulation (net vorticity). In the vorticity field, the isolation of a monopole is manifested by the presence of a *shield*—a ring of vorticity of common sign surrounding the central domain where the vorticity is oppositely signed. The stability or otherwise of a circular isolated monopole depends on its velocity profile. In monopoles possessing one shield, the critical factor is the steepness of the outer front of this profile, i.e., (in compact monopoles) the relative width of the shield. At moderate steepness, the monopole is linearly unstable, azimuthal mode 2 having the highest growth rate. The development and subsequent nonlinear saturation of this mode result in the formation of an isolated tripole [4,5,11,20,21], which is compact if the original monopole is compact.

Shortly after the first laboratory observations, a mesoscale tripole eddy was observed in the Bay of Biscay [22] with the use of satellite imaging. In the context of 2D flows, magnetized ion plasma and electron gas are equivalent to ordinary rotating fluids since the Lorentz force has the same effect as the Coriolis force. Therefore, it is little wonder that tripole vortices were soon observed with electron columns confined in Malmberg-Penning traps [12,13] and, recently, in magnetized plasma with the high-density plasma experiment (HYPER-I) device [14]. One can expect that optical tripoles will also be found (optical monopoles and dipoles in a homogeneous bulk medium are discussed in Ref. [23]).

The experimental detection of tripoles attests to their sufficient durability. This stimulates a search for explicit tripole solutions (e.g., for the purpose of a thorough stability analysis). In this paper, we construct semianalytical 2D solutions that are able to reproduce the main features of the observed tripoles.

II. EXPERIMENTAL EVIDENCE

A tripole emerged from a stirring-induced monopole in one of our f-plane laboratory experiments is displayed in Fig. 1(a), visualized by a fluorescent dye. It is a coherent vortex structure with three aligned patches of distributed vorticity—a core of positive vorticity and two weaker "satellites" of negative vorticity, the integral vorticity of the core

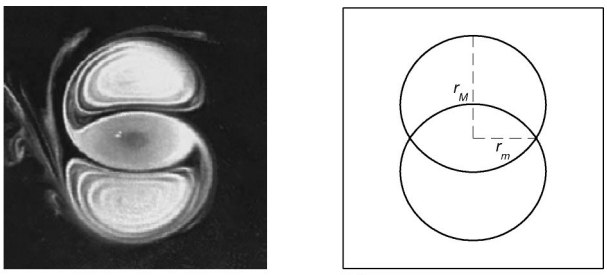

FIG. 1. Experimental tripole: (a) dye image; (b) sketch of the separatrix (r_M, maximal radius; r_m, minimal radius).

*Electronic address: zinovyk@mail.biu.ac.il

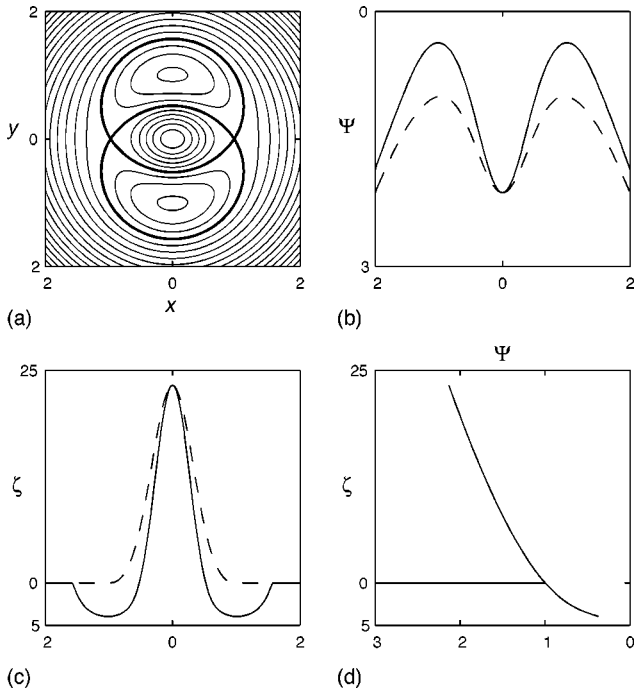

FIG. 2. Smooth two-mode tripole solution: (a) flow pattern (isocontours of Ψ and ζ; bold line, separatrix); (b) streamfunction cross sections at $x=0$ (solid line) and $y=0$ (dashed line); (c) vorticity cross sections at $x=0$ (solid line) and $y=0$ (dashed line); (d) scatter plot of ζ vs Ψ (straight line, exterior; curved line, interior).

being twice as strong (in absolute value) as that of each satellite. The tripole rotates counterclockwise in a solid-body-like manner exhibiting central symmetry; it is almost symmetric about the longitudinal axis passing through the poles of the vortex triple. The observed tripoles decay slowly mainly through the entrainment and dissipation. The time scale of this decay is much larger than the turnover time, so that the tripole evolution can be reckoned as "adiabatic." Thus, to study the form and structure of the tripole, we can consider the tripole in a co-rotating frame of reference as a stationary 2D flow of an ideal fluid. Under these assumptions, each fluid parcel keeps its vorticity, and the paths of parcels coincide with the streamlines. Note that the frontier Γ of the nonzero-vorticity area is a part of one of these contours.

In Fig. 1(a) two thin filaments linking the core with the satellites are seen. In the co-rotating frame, they mark the streamline that partially coincides with the core edge, where the particles move counterclockwise, and partially with the outer satellite edges (i.e., with Γ), where the movement is clockwise. Thus there are two centrally symmetric stagnation points at this streamline, where the velocity changes its direction. It is straightforward to see that these are the saddle points of the flow, and the streamline is a separatrix. It is possible approximately to identify the separatrix and, hence, the form of the vortex frontier Γ and the positions of the two saddle points by assuming the symmetry of the dye image about the longitudinal axis and performing the corresponding symmetry transformation [Fig. 1(b)]. Note that the central symmetry and the symmetry about the longitudinal axis together imply the symmetry about the transverse axis. The existence of the two symmetrical boundary corners will form one of the conditions for the determination of the tripole's shape and structure. In all our experiments, whenever the tripole was well formed, the border aspect ratio r_M/r_m [see Fig. 1(b) for notations], was fairly close to 1.60 (to within a 1.5% measurement error) regardless of the tripole size and intensity. This suggests the virtual similarity of the tripoles observed.

III. EQUATIONS AND BOUNDARY CONDITIONS

A. Definitions and notations

Consider now a compact isolated vortex bounded by a contour Γ and *steadily* rotating at a constant angular velocity ω. In a fixed frame of reference, the Lagrangian vorticity conservation is given by the equation

$$\partial\zeta/\partial t + J(\psi,\zeta) = 0,$$

where ψ and $\zeta=\Delta\psi$ are the streamfunction and vorticity, respectively; J is the Jacobian; Δ, Laplacian. In this frame supplied with polar coordinates r and $\tilde{\theta}$ with the origin in the center of rotation, ψ depends on r and $\theta=\tilde{\theta}-\omega t$ only. Thus, in the co-rotating frame with polar coordinates r and θ, the vortex is stationary, and we have

$$J(\Psi,\zeta) = 0, \quad \Psi = \psi - \tfrac{1}{2}\omega r^2,$$

where Ψ is the streamfunction in this frame. Stationarity implies $\Psi|_\Gamma = C = \text{const}$, so that Γ is a part of the separatrix streamline $\Psi = C$ whose self-intersection (stagnation) points are the corner vertices.

It is appropriate now to change to nondimensional variables. As will be seen below, for the solution to exist, the constants C and ω must be opposite in sign. Assuming (for definiteness) that the tripole rotates counterclockwise, i.e., $\omega>0$ and $C<0$, we choose the positive constants $-C$ and ω as the scales for the streamfunctions (ψ,Ψ) and vorticity, respectively, and $(-C/\omega)^{1/2}$ as the length scale. In what follows, x,y,r—the Cartesian coordinates and polar radius in the co-rotating frame of reference, and ψ, Ψ, ζ are nondimensional, while the interior (inside Γ) and exterior (outside Γ) streamfunctions and vorticity are marked with the superscripts (In) and (Ex), respectively.

B. Exterior problem

The requirements of compactness and isolation of the vortex provide the following relationships:

$$\Delta\psi^{(Ex)} = 0; \quad \psi^{(Ex)} \to 0 \quad \text{as} \quad r \to \infty. \tag{1}$$

The condition at the boundary Γ is:

$$\Psi^{(Ex)}|_\Gamma = -1. \tag{2}$$

Given the contour Γ, relationships (1) and (2) determine a unique exterior solution. Conversely, by prescribing a specific form of the exterior solution, the family of possible borders is fixed. We choose the second alternative and consider solutions to (1) that are symmetric about the x and y

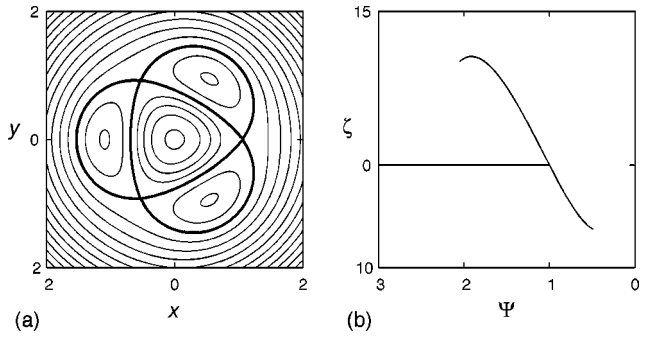

FIG. 3. Smooth two-mode quadrupole solution: (a) flow pattern; (b) scatter plot of ζ vs Ψ [details as in Figs. 2(a) and 2(d)].

axes (in the co-rotating frame) and incorporate a finite number M of azimuthal modes

$$\Psi^{(Ex)} = \frac{1}{2}\left[\sum_{\mu=1}^{M} a_{2\mu}\frac{1}{r^{2\mu}}\cos(2\mu\theta) - r^2\right], \tag{3}$$

where $a_{2\mu}$ are constants. Based on the above experimental observations, relationships (2) and (3) must be supplemented with stagnation-point (corner) conditions. The r coordinate of a boundary point is a function of θ; it will be denoted by $r_\Gamma = r_\Gamma(\theta)$. Without loss of generality we can fix the orientation of the tripole so that the points $\theta=0$, $r=r_\Gamma(0)$ and $\theta=\pi$, $r=r_\Gamma(\pi)$ are the boundary corner vertices, i.e., $r_\Gamma(0)=r_\Gamma(\pi)=r_m$ [see Fig. 1(b)]. Due to the symmetry of the tripole, it is sufficient to impose the corner conditions on only one of these points, say, on $\theta=0$, $r=r_m$:

$$\Psi^{(Ex)}\big|_{\theta=0,r=r_m} = -1, \qquad \frac{\partial}{\partial r}\Psi^{(Ex)}\bigg|_{\theta=0,r=r_m} = 0. \tag{4}$$

Relationships (2)–(4) serve to determine the tripole frontier.

C. Interior problem

The interior problem involves the third-order equation

$$J(\Psi^{(In)}, \Delta\Psi^{(In)}) = 0 \tag{5}$$

and the boundary conditions

$$\Psi^{(In)}\big|_\Gamma = -1, \qquad \partial\Psi^{(In)}/\partial n\big|_\Gamma = \partial\Psi^{(Ex)}/\partial n\big|_\Gamma, \tag{6}$$

where n is the boundary normal. When dealing with the interior, we assume the border and exterior solution to be completely known. This determines the interior solution, including the relation between the vorticity and streamfunction that exists due to Eq. (5) and is nonlinear in noncircular multipolar vortices [24,25]. The interior is solved with the use of Newton-Kantorovich iterative algorithm. The streamfunction at iteration $i+1$ is represented as $\Psi^{(In)}_{i+1} = \Psi^{(In)}_i + \delta$, and the correction δ is found from the linearized version of Eq. (5),

$$J(\delta, \Delta\Psi^{(In)}_i) + J(\Psi^{(In)}_i, \Delta\delta) = -J(\Psi^{(In)}_i, \Delta\Psi^{(In)}_i),$$

and boundary conditions (6) written in terms of δ. To solve the linear problem we apply a collocation method with a polynomial representation of the correction, $\delta = \sum_{0\le p+s\le N}\alpha_{p,s}x^{2p}y^{2s}$, where N is some preset integer (due to the symmetry of the tripole about the x and y axes, only even powers of x and y are present in this polynomial); the initial guess $\Psi^{(In)}_i$ is also given in a polynomial form. This allows us to calculate in polynomials all the differential operators and reduce the problem to a system of linear equations in $\alpha_{p,s}$ (corresponding to a chosen set of interior and boundary points $K \gg N$), which is solved numerically in the least-squares sense (for technical details see Ref. [24]). As soon as the interior solution is found, the $\zeta^{(In)}$ vs $\Psi^{(In)}$ relation is computed.

Due to the dependence of $\zeta^{(In)}$ on $\Psi^{(In)}$, the streamlines and iso-vorticity contours (i.e., the iso-contours of $\Psi^{(In)}$ and $\zeta^{(In)}$) coincide. Thus the interior vorticity along the vortex border, $\zeta^{(In)}|_\Gamma$, is constant but not necessarily zero. This means that, in general, there is a vorticity jump across the border. We will show, however, that a solution with no vorticity jump does exist.

IV. TRIPOLE SOLUTIONS

Confining ourselves to the tripoles that contain not more than two exterior modes, we put $M=2$. Relationships (2) and (3) yield the equation

$$r_\Gamma^6 - 2r_\Gamma^4 - a_2 r_\Gamma^2\cos 2\theta - a_4\cos 4\theta = 0$$

which, with some restrictions on the parameters a_2 and a_4, determines closed contours $r_\Gamma - r_\Gamma(\theta)$. (Note that the equation $r_\Gamma^6 + 2r_\Gamma^4 - a_2 r_\Gamma^2\cos 2\theta - a_4\cos 4\theta = 0$ resulting from the condition $C/\omega > 0$ has no real roots for some values of θ, whatever the parameters $a_2 \neq 0$ and a_4.) The stagnation-point conditions (4) provide two constraints that allow us to express parameters a_2 and a_4 in terms of r_m and choose r_m as the only free parameter,

$$a_2 = r_m^2(3r_m^2 - 4), \quad a_4 = r_m^4(1 - r_m^2). \tag{7}$$

Thus the two-mode tripole solutions constitute a one-parameter family.

The simplest tripole, corresponding to the case $M=1$, is obtained by setting $r_m=1$ in Eqs. (7). In this case, $a_2=-1$, $a_4=0$, and $r_\Gamma = \sqrt{1+\sqrt{1-\cos 2\theta}}$. The boundary aspect ratio in the one-mode tripole, $r_M/r_m = \sqrt{1+\sqrt{2}} \approx 1.554$, is rather close to the observed value, but computations show that there is a vorticity jump across the border: $\zeta^{(In)}|_\Gamma \approx -1.25$. In contrast, the observed tripoles are essentially smooth in this respect [8]. Moreover, one may surmise that continuity of vorticity is critical for vortex stability [24,26].

Further computations with varying r_m disclose that $\zeta^{(In)}|_\Gamma$ is a monotonic function or r_m, changing sign at $r_m \approx 0.97$. Thus, we conclude that there exists a unique smooth two-mode tripole solution. We note that the weight of the 4th harmonic in this solution is relatively small ($-a_4/a_2 \approx 0.10$) and inclusion of higher even harmonics in Eq. (3) barely changes the result. In dimensional variables the two-mode smooth tripoles differ only in size and angular velocity (i.e., in amplitude), their aspect ratio, $r_M/r_m \approx 1.61$, being extremely close to the experimentally estimated value of 1.60.

The smooth two-mode solution is shown in Fig. 2. Its flow pattern [Figs. 2(a) and 2(b)] closely follows the experimental pattern (Fig. 1(a); cf. also Fig. 13 in Ref. [8] and Fig. 7 in Ref. [4]); also the vorticity distribution [Figs. 2(a) and 2(c)] resembles that in the experiments and computer simulations (cf. Fig. 6 in Ref. [8] and Fig. 8 in Ref. [4]). The vorticity-streamfunction relationship [Fig. 2(d)] is in good agreement with that in the experimental tripoles (cf. Fig. 12 in Ref. [8]): in the interior, it is convex downwards, being basically linear in the central part of the core but clearly nonlinear in the satellites.

V. DISCUSSION

In some aspects, the solutions presented above can be regarded as an extension of the classical ideas of Lamb and Chaplygin. Indeed, in the classical circular dipole solution only one lowest azimuthal mode ($\sin\theta$ or $\cos\theta$) is present. Likewise, the simplest of our tripole solutions bears only one lowest mode ($\cos 2\theta$) in the exterior. The uniqueness of the smooth two-mode tripole and the fact that the solution incorporates the minimal number of the lowest exterior modes required to remove any vorticity jump also make it allied to the Lamb-Chaplygin dipole. Furthermore, based on the same logic, i.e., prescribing the form of the exterior solution and demanding the existence of 3, 4, etc., stagnation points, and using essentially the same numerical technique, higher-order one- and two-mode multipoles—quadrupole, pentapole, etc.—can be obtained. An example is the smooth quadrupole solution bearing two lowest harmonics ($\cos 3\theta$ and $\cos 6\theta$) in the exterior (Fig. 3). Its close similarity to the "triangular" vortex obtained in numerical simulations [10] becomes obvious when we bring in correspondence the definitions of the streamfunction and vorticity assumed here and in Ref. [10] ($\Psi \to -\Psi, \zeta \to -\zeta$) and compare our Fig. 3 with Figs. 9 and 10 in Ref. [10].

It is our opinion that the strategy followed in the construction of a tripole solution may find use in various fields of nonlinear dynamics where the search for localized structures is the issue.

ACKNOWLEDGMENTS

This research was supported by the Israel Science Foundation (Grant No. 616/00), US-Israel Binational Science Foundation (BSF, Grant No. 2002392) and the J. M. Burgers Centre, The Netherlands. Z. K. acknowledges the hospitality extended to him by the Fluid Dynamics Laboratory of Eindhoven University of Technology, The Netherlands, where the experimental part of the work was done, and thanks G. J. F. van Heijst and R. R. Trieling for sharing with him their experience in vortex production. Discussions with G. J. F. van Heijst, B. Legras, V. M. Gryanik, M. Sokolovsky, V. Shrira, and V. Zeitlin were helpful. We are grateful to I. White whose comments led to improvements of this paper.

[1] H. Lamb, *Hydrodynamics*, 2nd ed. (Cambridge University Press, Cambridge, England, 1895).
[2] S. A. Chaplygin, Trans. Phys. Sect. Imperial Moscow Soc. Friends of Natural Sci. **11** (2), 11 (1903) (in Russian).
[3] V. V. Meleshko and G. J. F. van Heijst, J. Fluid Mech. **272**, 157 (1994).
[4] B. Legras, P. Santangelo, and R. Benzi, Europhys. Lett. **5**, 37 (1988).
[5] X. J. Carton, G. R. Flierl, and L. M. Polvani, Europhys. Lett. **9**, 339 (1989).
[6] G. J. F. van Heijst and R. C. Kloosterziel, Nature (London) **338**, 569 (1989).
[7] R. C. Kloosterziel and G. J. F. van Heijst, J. Fluid Mech. **223**, 1 (1991).
[8] G. J. F. van Heijst, R. C. Kloosterziel, and C. W. M. Williams, J. Fluid Mech. **225**, 301 (1991).
[9] J. P. Hesthaven *et al.*, Phys. Fluids A **5**, 1674 (1993).
[10] G. F. Carnevale and R. C. Kloosterziel, J. Fluid Mech. **259**, 305 (1994).
[11] X. Carton and B. Legras, J. Fluid Mech. **267**, 53 (1994).
[12] T. B. Mitchell and C. F. Driscoll, Phys. Rev. Lett. **73**, 2196 (1994).
[13] X.-P. Huang, K. S. Fine, and C. F. Driscoll, Phys. Rev. Lett. **74**, 4424 (1995).
[14] A. Okamoto *et al.*, Phys. Plasmas **10**, 2211 (2003).
[15] L. M. Polvani, and X. J. Carton, Geophys. Astrophys. Fluid Dyn. **51**, 87 (1990).
[16] Y. G. Morel and X. J. Carton, J. Fluid Mech. **267**, 23 (1994).
[17] H. E. Cabral and D. S. Schmidt, SIAM J. Math. Anal. **31**, 231 (1999).
[18] D. Crowdy and M. Cloke, Phys. Fluids **15**, 22 (2003).
[19] V. F. Kozlov, Oceanology (Engl. Transl.) **34**, 10 (1994).
[20] P. R. Gent and J. C. McWilliams, Geophys. Astrophys. Fluid Dyn. **35**, 209 (1986).
[21] G. R. Flierl, J. Fluid Mech. **37**, 349 (1988).
[22] R. Pingree and B. Le Cann, Deep-Sea Res., Part A **39**, 1147 (1992).
[23] J. J. Garsia-Ripoll *et al.*, Phys. Rev. Lett. **85**, 82 (2000).
[24] Z. Kizner, D. Berson, and R. Khvoles, J. Fluid Mech. **489**, 199 (2003).
[25] J. P. Boyd and H. Ma, J. Fluid Mech. **221**, 597 (1990).
[26] N. Paldor, J. Phys. Oceanogr. **29**, 1442 (1999).